Detection of 2,4-Dinitrotoluene by Metal-Graphene Hybrid Plasmonic Nanoantennas with a Golden Ratio Rectangular Resonator

Ahmet Murat Erturan[1], Seyfettin Sinan Gultekin[1], Habibe Durmaz[2, *]

[1]*Department of Electrical Electronics Engineering, Konya Technical University,*
Konya, Turkey
[2]*Department of Electrical Electronics Engineering, Karamanoglu Mehmetbey University,*
Karaman, Turkey
a.muraterturan@gmail.com; ssgultekin@ktun.edu.tr; *durmazgul@gmail.com

Abstract—**Plasmonic nanoantenna arrays have become increasingly popular for the detection of chemical molecules, biomolecules, viruses, and agents. In this study, our objective was to detect explosive-based 2,4-dinitrotoluene (2,4-DNT) with a metal-graphene hybrid plasmonic rectangular nanoantenna with a golden ratio size formed by choosing two consecutive numbers from the Fibonacci series. The golden rectangular resonator provides nearly perfect absorption without the need for impedance matching calculations and complex optimisation algorithms. In surface enhanced infrared absorption (SEIRA) applications, the internal losses of metallic nanostructures degrade their sensing performance. To improve performance sensitivity, graphene with high electrical conductivity and electrical tunability was used. The spectral fingerprints of 2,4 DNT at 6300 nm, 6580 nm, and 7500 nm were enhanced with a metal-graphene hybrid structure. The biosensor platform introduced, by combining the graphene and nanoantennas with a golden ratio and by adjusting the Fermi energy level of graphene, can be beneficial for highly sensitive tunable biosensors for a broad spectrum to identify the molecular fingerprints of specific biomolecules.**

Index Terms—**Plasmonic nanoantenna; Surface enhanced infrared absorption (SEIRA); 2,4-dinitrotoluene (2,4-DNT); Golden ratio; Fibonacci series.**

I. INTRODUCTION

Plasmonic metamaterials are artificial materials that exhibit extraordinary optical properties in sub-wavelength particles [1]. Due to the oscillating plasmons along the surface between the metallic nanoparticles and the dielectric material, they trap the electromagnetic field and become extremely sensitive to the dielectric permeability of the environment surrounding the structure [2]. Therefore, they have been widely used in areas such as biomolecular [3] and chemical sensing [4], defence technology [5], and photodetector [6]. The infrared spectrum is the region where molecules have specific fingerprints, allowing non-invasive and label-free detection with plasmonic structures. However, the size of nanoparticles is too small (~ nanometer) compared to the wavelength of light, which brings a low signal-to-noise ratio and poses a disadvantage

for sensitive detection. This problem has led to the development of the surface enhanced infrared absorption (SEIRA) method, which takes advantage of wide optical field enhancement near metallic nanostructures. With this method, small amounts of molecules can be detected. However, the field limitation and high internal losses of plasmons developed at the metal-dielectric interface are disadvantages in SEIRA applications. A strong enhancement of optical fields is needed to spectrally observe the absorption deeps caused by specific fingerprints of molecules. In recent years, graphene has become an important material for sensing due to its high electrical conductivity, electrical tunability, and thermal conductivity in terahertz and infrared applications [7]. Furthermore, this 2D carbon allotrope, when used with a metal nanostructure, significantly amplifies the absorption signals of the vibrational modes of the molecules and can strongly detect these modes in mid-infrared sensing [8], [9]. The resonance mode of the graphene nanoantenna can be electrically tuned to different wavelengths of operation to detect the fingerprints of molecules [10].

Plasmonic metamaterials can be independently tuned with electrical and magnetic resonances, by matching their impedance with the impedance of the free space and reducing the reflection of the incoming electromagnetic wave to zero ($z = \mu/\varepsilon = 1$) [11]. To satisfy impedance matching, complex impedance matching calculations or simulation trials are required. In recent years, structures that are compatible with the Fibonacci series and have the golden ratio have been presented in various antenna applications covering the radio frequency (RF) and microwave frequency regions, and effective results have been obtained [12]–[14]. Any number in the Fibonacci series is the sum of the previous two numbers, and as the numbers get larger, the ratio of two consecutive numbers approaches the golden ratio. After the 13th number of the series, the golden ratio is constant and equal to the ratio of both consecutive numbers.

The aim of this paper is to detect 2,4-dinitrotoluene (2,4-DNT), which is the main production ingredient of 2,4,6-trinitrotoluene (TNT), one of the nitroaromatic (NAC)

compounds and explosives. DNT is the primary material for TNT production and often exhibits contamination indicating the presence of TNT [15]. Especially during production and packaging, waste at facilities, unexploded ordnance, and land-sea mines are the main causes of this pollution [16]. 2,4-DNT has been shown to cause highly toxic mutagenic reactions in humans and animals and has been classified as a carcinogenic compound and listed as the main pollutant by the U.S. Environmental Protection Agency (EPA) [16], [17]. Explosives are usually detected using gas chromatography mass spectrometry (Gc-MS), high liquid pressure chromatography (HPLC), and other analytical methods, where these methods require many pre-processes such as analysis and extraction [18], [19]. Label-free and sensitive detection of DNT and TNT without pre-processing is crucial for military, civil, and environmental areas.

In this study, the detection of DNT by the SEIRA spectroscopy method was carried out using a plasmonic metal-graphene hybrid structure where the golden ratio is implemented on the dimensions of the plasmonic antennas for the first time. In the design, the rectangular-shaped plasmonic antennas are used for simplicity with the golden ratio between the sides of the rectangles without the need to satisfy impedance matching criteria to obtain 95 % absorption of the incoming electromagnetic radiation. In addition, by changing the side lengths of the rectangle, the golden ratios are obtained at different values and the static tunability of the SEIRA platform is shown. Furthermore, the dynamic tunability of the SEIRA system has been demonstrated by varying the Fermi energy level of the graphene layer in the metal-graphene hybrid structure. Dynamic tunability offers the luxury of setting the resonance frequency to any desired value by only changing the Fermi level instead of changing the geometric dimensions of the antenna during manufacturing as in the case of static tuning, therefore, reducing the fabrication cost. These numerical results of the proposed hybrid SEIRA platform show three different vibrational fingerprints of 2,4-DNT in the mid-IR region. Our numerical results show that a label-free detection of 2,4-DNT can be achieved with our proposed system. Therefore, the detection of DNT will prevent the widespread environmental threat.

II. ABSORPTION CAPACITY OF SEIRA PLATFORM BASED ON GOLDEN RATIO RECTANGULAR NANOSTRUCTURE

The model structure and absorption spectrum of the proposed SEIRA system are shown in Fig. 1. The SEIRA platform consists of 200 nm (h_3) thick gold (Au) film at the bottom layer to act as a mirror to block optical transmission. In addition, there is a 100 nm (h_2) thick MgF_2 dielectric material and a single layer of graphene, respectively. In the upper layer, there is a rectangular Au resonator with a golden ratio ($l_x/l_y = 1.618$) with lengths $l_x = 1597$ nm and $l_y = 987$ nm in the x- and y-directions, respectively (Fig. 1(a)). The optimal thicknesses of each layer are $h_1 = 50$ nm, $h_2 = 100$ nm, and $h_3 = 200$ nm, respectively (Fig. 1(b)). The dielectric coefficients of the materials are taken from Palik [20].

Electromagnetic simulations were performed using the finite differences time domain (FDTD) programme. The periodic boundaries of the plasmonic structure were set as $P_x = P_y = 2500$ nm in the x- and y-directions. The structure was illuminated with linear polarised light along the x-axis at normal incidence, and perfectly matched layers (PML) were used in the z-direction to prevent unwanted backscattering of electromagnetic fields. The single-layer graphene was modelled with the Kubo formula in (1) and (2) [21]–[23]:

$$\sigma(\omega) = \sigma_{\mathrm{intra}}(\omega) + \sigma_{\mathrm{inter}}(\omega), \tag{1}$$

$$\sigma(\omega)_{\mathrm{intra}} = \frac{e^2 k_B T}{\pi \hbar^2} \frac{i}{\omega + i r^{-1}} \left[\frac{\mu_c}{k_B T} + 2\ln(e^{-\mu_c/k_B T} + 1) \right], \tag{2}$$

where ω is the angular frequency, τ is the relaxation constant of the Drude model, e is the electron charge, $\hbar = h/2\pi$ is the reduced Planck's constant, k_B is the Boltzmann's constant, μ_c is the chemical potential (set as 0.25 eV), and T is the temperature in Kelvin (set as 300 K), respectively.
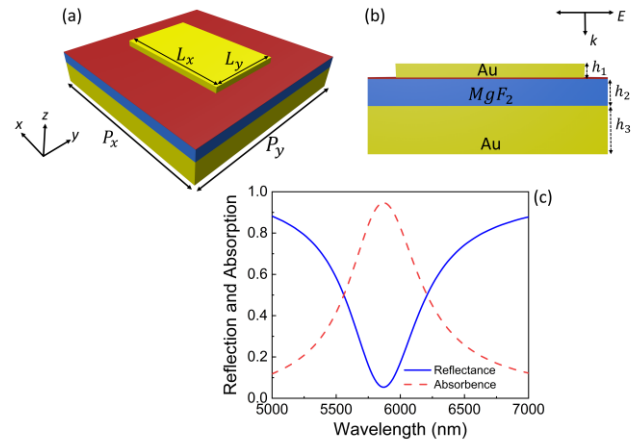
Fig. 1. Schematic of plasmonic nanoantennas with golden ratio: (a) Top view; (b) Side view; (c) Reflection and absorption spectra of the proposed SEIRA system.

The lengths l_x and l_y of the gold resonator are determined as the 18th and 17th numbers of the Fibonacci series (1597 nm and 987 nm), respectively. Figure 1(c) shows the absorption and reflection spectra of the plasmonic structure with the golden ratio. Based on this figure, the rectangular Au structure designed with the golden ratio exhibits remarkable absorption of 95 % at the resonance wavelength (5887 nm). The physical origin of this resonance behaviour of the nanoscopic metallic antenna has been analytically studied by Zheng, Vandenbosch, and Moshchalkov [24]. Figure 1(c) shows that the strong and stable resonance mode can be obtained successfully by implementing golden ratios on the side lengths of the resonator without the need to satisfy the equivalent impedance, which is a timely and costly optimisation process.

To show the strong field enhancement due to the graphene layer, the enhancement of the electric field intensity and charge distributions of the nanoantennas are further investigated with the same programme as shown in Fig. 2(a) and Fig. 2(b). In Fig. 2(c) and Fig. 2(d), the same electric field and charge distributions are shown in the

absence of the graphene layer. When the electric field and charge distributions are compared from Fig. 2(a) and Fig. 2(c), there are sharp edges in the field distributions in the graphene layer indicating more field enhancement and therefore more absorption at that specific resonance wavelength. In both graphene and metal hybrid structures, uniform fields are localised at the corners and along the short sides. The strong field enhancement in the proposed SEIRA platform has been proven by the effect of both graphene and antenna plasmons on the metal-graphene hybrid structure. Figure 2(b) and Figure 2(d) are charge densities at the metal-graphene and metal-dielectric interfaces. The density of charge is responsible for the performance of the SEIRA system since the incoming electromagnetic wave interacts with charges at the nanoscale. Higher charge density may cause a stronger interaction with light, but it may also make the antenna more susceptible to noise and other disturbances. In both charge density graphs, the charges with different polarities are located at the antenna edges, creating a dipole that leads the incoming wave to be polarised in the y-direction. In Fig. 2(b), the charge distribution of the proposed metal-graphene hybrid structure has two orders of magnitude compared to the metal hybrid structure as shown in Fig. 2(c) due to the excellent electrical conductivity of graphene and the strong electrical field confinement properties.
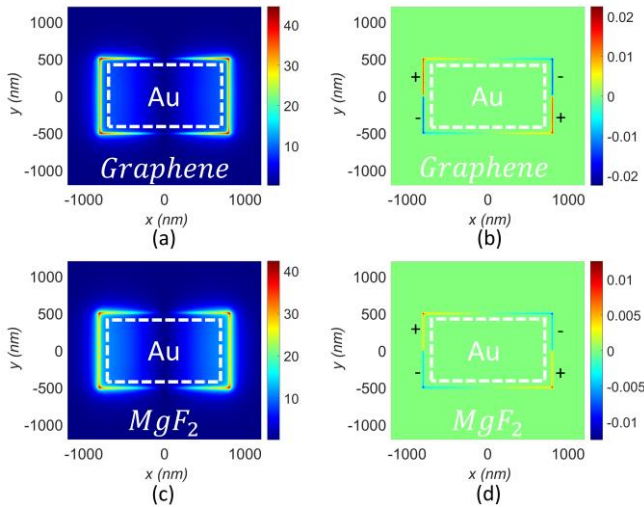
Fig. 2. (a) Distribution of the electric field of the metal-graphene hybrid structure; (b) Charge density of the metal-graphene hybrid structure; (c) Distribution of the electric field of the metal structure; (d) Charge density of the metal structure. In both cases, the dimensions of the golden ratio rectangular resonator are $l_x = 1597$ nm, $l_y = 987$ nm. The Fermi energy level of graphene is 0.25 eV.

The static tunability of the metal hybrid structure was investigated by keeping the golden ratio by varying the side lengths of the rectangular antennas. The l_x- and l_y-values were chosen as two consecutive numbers from the Fibonacci series (18th and 17th numbers). Different combinations of l_x- and l_y-values were chosen to form the golden ratio, and these values were defined as GR (golden ratio) as depicted in Table I.

According to the Table I, l_x and l_y values are adjusted to maintain a constant golden ratio relationship between l_x and l_y variables, and each variable parameter is expressed as GR

(GR-1, GR-2, GR-3, etc.). Figure 3(a) shows the reflectance spectrum obtained from different l_x- and l_y-parameters given in Table I as GR kept constant. The varying l_x and l_y dimensions such that the golden ratio is satisfied, the similar absorption spectra are obtained at different resonance wavelengths. In Fig. 3(b), these absorption and peak wavelength values are shown graphically. As l_x- and l_y-values increase, the resonance mode redshifts linearly with a decrease in the absorption strength from GR-1 to GR-5. The proposed rectangular resonator with a golden ratio gives at least a minimum of 90 % reflection. This is a great advantage in the design of the plasmonic structure. The dynamic tunability of the plasmonic structure shows that this structure can be used in sensor, detector, and filter applications, etc.

TABLE I. GOLDEN RATIO VARIABLES OF DIFFERENT L_X- AND L_Y-PARAMETERS.

Variable	l_x	l_y	Ratio
GR-1	1400 nm	865 nm	1.618
GR-2	1500 nm	927 nm	1.618
GR-3	1597 nm	987 nm	1.618
GR-4	1700 nm	1050 nm	1.618
GR-5	1800 nm	1112 nm	1.618
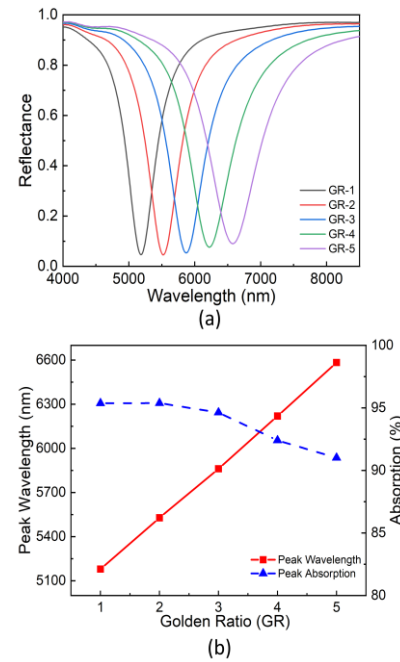
Fig. 3. (a) The spectral response of the SEIRA platform as golden ratio (GR) parameters ranging from GR-1 to GR-5; (b) The spectral shifts of the resonance peak and the absorption peak of the plasmonic antennas with parameters ranging from GR-1 to GR-5. The Fermi energy level for graphene is taken as 0.25 eV at each spectrum.

The electrical tunability of the metal-graphene hybrid structure is shown by changing the Fermi energy level from 0.1 eV to 0.4 eV as shown in Fig. 4. As the Fermi energy increases, the resonance frequency redshifts as expected. The absorption is strongest (95 %) for the Fermi energy of 0.25 eV and gradually decreases toward 0.4 eV. However, about 90 % absorption for the 0.4 eV Fermi energy can be obtained, as shown in Fig. 4(b). The dynamic tunability of the graphene hybrid structure gives an important advantage over the metal hybrid structure, as the operating frequency

can be adjusted after manufacturing for the identification of the different molecules. The SEIRA platform can be dynamically tunable as the Fermi energy [eV] changes without causing a large loss in the absorption peak.
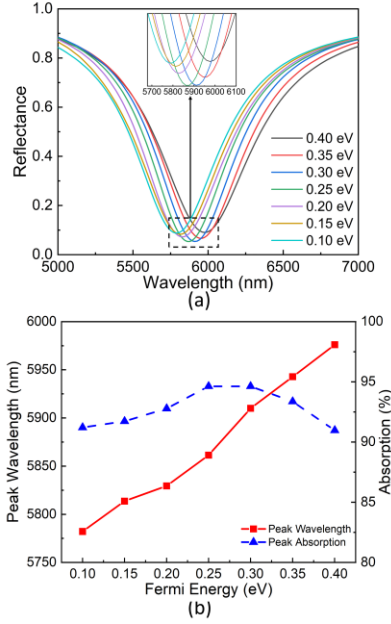
Fig. 4. (a) Absorption spectra of the graphene hybrid SEIRA platform with varying Fermi energy from 0.1 eV to 0.4 eV; (b) Change in resonance wavelength and absorption strength with the change in Fermi energy.

III. SEIRA DETECTION OF 2,4-DINITROTOLUENE

2,4-dinitrotuluene (2,4-DNT) is one of the primary ingredients used in the production of TNT explosives and is a highly dangerous chemical. It is not only a military, but also a serious environmental pollutant. In this study, the detection of 2,4-DNT using the SEIRA method was carried out numerically with a plasmonic nanoantenna structure. In SEIRA spectroscopy, the vibrational modes of the molecules overlap with the resonance frequencies of the plasmonic antennas. Therefore, in this method, absorption deep-caused by the vibrational modes of the target molecules in the absorption spectrum of the plasmonic antennas is detected. It is known that 2,4-DNT gives spectral signatures at three different wavelengths, approximately 6300 nm, 6580 nm, and 7500 nm in the infrared region [25]. To show the SEIRA capacity of the plasmonic structure, the 3-oscillator Drude-Lorenz model of 2,4-DNT was used (3)

$$\varepsilon(\omega) = \varepsilon_\infty + \sum_{t=1}^{3} X_t \omega_{0,t}^2 / (\omega_{0,t}^2 - \omega^2 - j\omega\gamma_t), \qquad (3)$$

where $\varepsilon_\infty = 2.1901$ is the high-frequency constant, the oscillation frequency $\omega_{0,1} = 2.52 \times 10^{14}$ (rad/s), $\omega_{0,2} = 2.877 \times 10^{14}$ (rad/s), and $\omega_{0,3} = 3.011 \times 10^{14}$ (rad/s). The damping frequency $\gamma_1 = 3.74 \times 10^{12}$ (rad/s), $\gamma_2 = 4.115 \times 10^{12}$ (rad/s), and $\gamma_3 = 3.74 \times 10^{12}$ (rad/s) and oscillator amplitudes are $X_1 = 10^{-2}$, $X_2 = 7.4 \times 10^{-3}$, and $X_3 = 1.68 \times 10^{-3}$, respectively. Figure 5(a) and Figure 5(b) show the real and imaginary parts of the permittivity of the 2,4-DNT molecule obtained from the model separately.
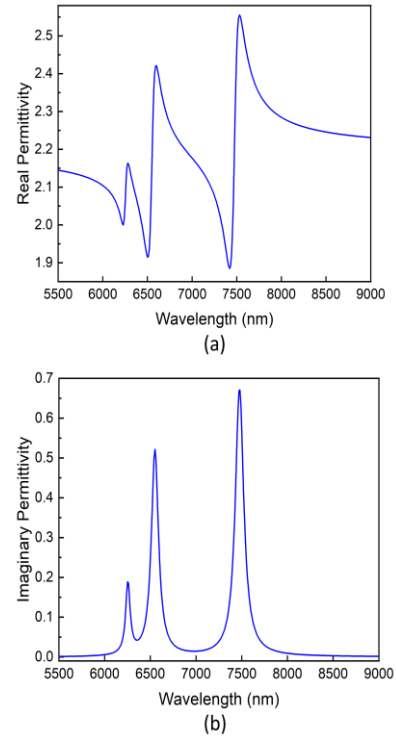
Fig. 5. (a) The real part of the permittivity of 2,4-DNT; (b) The imaginary part of the permittivity of 2,4-DNT.

In the numerical study, 2,4-DNT was considered as an 8 nm thick film on plasmonic structures. Depending on the changing GR values in Fig. 6(a) (Table I), three different spectral vibrational modes of 2,4-DNT were investigated. The spectral fingerprints of 2,4-DNT are shown with green, blue, and red bars at wavelengths of 6300 nm, 6580 nm, and 7500 nm, respectively. In the proposed SEIRA system, these vibrational modes of the 2,4-DNT molecule have been observed at different resonance modes by changing the l_x- and l_y-values as shown with different golden ratios in Fig. 6(b).
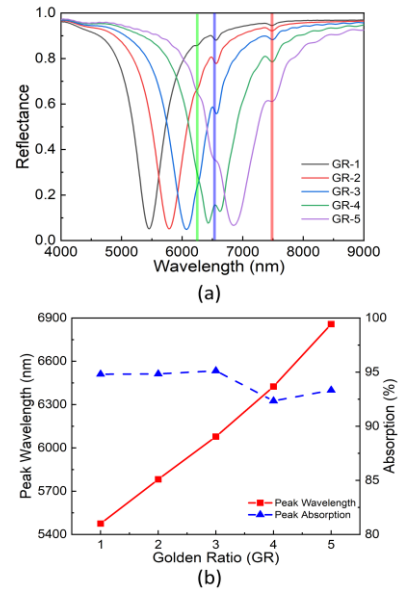
Fig. 6. (a) The reflectance spectra of the SEIRA platform consist of a metal hybrid structure. The spectral fingerprints of 2,4-DNT are marked with green, blue, and red bars at 6300 nm, 6580 nm, and 7500 nm, respectively; (b) The dependence of peak resonance wavelength and absorption strength on l_x- and l_y-parameters. The Fermi energy level for graphene is taken as 0.25 eV at each spectrum.

In this figure, the red line shows the wavelength of the resonance mode, whereas the blue line shows the absorption strength of the system. It is very clear that golden ratio rectangular resonators of different sizes achieve absorption of up to about 95 % just by keeping the golden ratio between the antenna's length instead of optimising all the impedance matching conditions. This leads to an easy and controllable fabrication of the sensors by justifying the experimental errors that may occur during manufacturing. At each GR value, the resonance wavelength of the sensor platform shifted to the longer wavelength, and it is compatible with Fig. 4. The three vibrational modes of 2,4-DNT are clearly observed as small deeps for each spectrum obtained from plasmonic antennas with the golden ratio. These results show that the proposed structure can be used for the label-free detection of different biological or chemical molecules.

Figure 7(a) and Figure 7(b) show the 2,4-DNT detection capacity of the SEIRA platform without and with graphene metasurface, respectively.
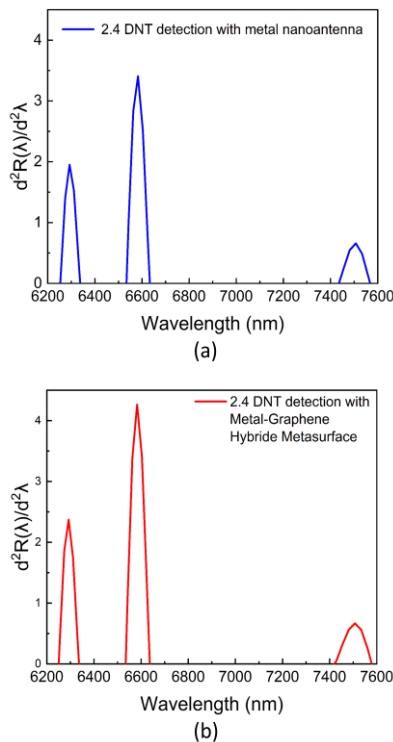
Fig. 7. The second derivatives of SEIRA signals of 2,4-DNT (a) with a metal-gold hybrid rectangular antenna with a golden ratio and (b) with a metal-graphene hybrid antenna with a golden ratio. The golden ratio resonator was created according to the GR-3 parameters in Table I. The graphene energy level is 0.25 eV.

To better emphasise the spectral depthsdue to the vibrational modes of 2,4-DNT in the absorption spectra for GR-3, the second derivative of the absorption is plotted as seen in Fig. 7(a) and Fig. 7(b). Figure 7(a) shows the second derivative of the absorption spectra of the metal-dielectric structure (without the graphene layer). In the same figure, the strength of the second derivative of the absorption peaks due to vibrational modes has an amplitude of about 2 at 6300 nm, 3.35 at 6580 nm, and 0.5 at 7500 nm. On the contrary, Fig. 7(b) shows the second derivative of the absorption spectra of the metal-graphene hybrid structure

for the Fermi energy level of 0.25 eV. Here it is clearly seen that the amplitudes of the peaks have increased. These amplitudes are about 2.4 at 6300 nm, 4.3 at 6580 nm, and 0.6 at 7500 nm. Although the highest absorption peak is expected at 7500 nm; however, the vibrational mode at this wavelength falls in the tail of the absorption spectrum. The results show that the SEIRA platform based on a metal-graphene hybrid structure has a better sensing performance compared to that of the SEIRA system based on a metal-dielectric.

Finally, 2,4-DNT detection was performed with different Fermi levels in a metal-graphene hybrid structure. As seen in Fig. 8, the resonance wavelength shifts to the longer wavelength side as the Fermi level increases.
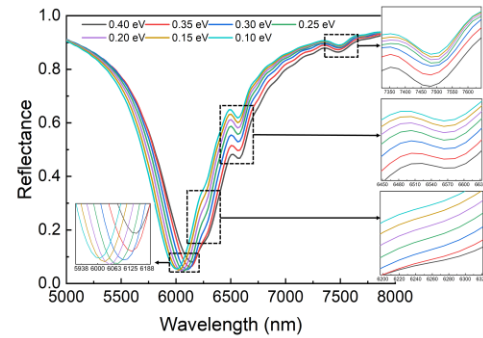
Fig. 8. Reflection spectra of 2,4-DNT molecules by the SEIRA platform at Fermi energy levels ranging from 0.1 eV to 0.4 eV. Spectral fingerprints are marked at 6300 nm, 6580 nm, and 7500 nm at each Fermi level.

The three molecular fingerprints of 2,4-DNT are observed at 6300 nm, 6580 nm, and 7500 nm in the absorption spectra at each Fermi level. These results show that our proposed SEIRA system based on rectangular antennas with/without a graphene layer can successfully detect the molecular fingerprints of 2,4-DNT.

IV. CONCLUSIONS

We show the detection of 2,4-DNT, an explosive and environmental pollutant, by the SEIRA platform consisting of a hybrid structure of a golden ratio rectangular plasmonic structure with graphene. 2,4-DNT has spectral fingerprints at 6300 nm, 6580 nm, and 7500 nm. The SEIRA platform has 95 % reflection that can be achieved with the proposed golden ratio rectangular structure by eliminating the long simulation and experimental work to satisfy the impedance matching. Also, the combination of graphene dynamic tunability via Fermi energy with the antennas (with a golden ratio) has given another freedom to change the resonance frequency of the system. The results show that the rectangular plasmonic structure with different antenna parameters chosen according to the golden ratio can detect three different spectral fingerprints of 2,4-DNT. In addition, detection of molecular fingerprints of 2,4-DNT with the metal-graphene hybrid structure was shown by changing the Fermi energy from 0.1 eV to 0.4 eV. This study offers an innovative contribution to the literature, featuring a geometric structure designed using two Fibonacci numbers, electrical tunability provided by a metal-graphene hybrid structure, and the capability to detect three distinct spectral fingerprints of 2,4-DNT. Our proposed SEIRA sensor

platform can be highly beneficial with the combination of graphene and nanoantennas with golden ratio dimensions and by adjusting the Fermi energy level of graphene for the detection of weak molecular fingerprints in a wide spectral range. Finally, this platform can be used in practical applications by minimising the fabrication errors caused by the length of the antennas simply by keeping the golden ratio between the lengths of the rectangular-shaped antenna.

CONFLICTS OF INTEREST

The authors declare that they have no conflicts of interest.

REFERENCES

[1] Y. Y. Lee, R. M. Kim, S. W. Im, M. Balamurugan, and K. T. Nam, "Plasmonic metamaterials for chiral sensing applications", *Nanoscale*, no. 1, 2020. DOI: 10.1039/C9NR08433A.

[2] G. G. de la Cruz and M. Oliva-Leyva, "Plasmon resonances of graphene-dielectric-metal structures calculated by the method of recurrence relations", *Plasmonics*, vol. 16, pp. 2259–2267, 2021. DOI: 10.1007/s11468-021-01466-x.

[3] N. Zhang *et al.*, "High sensitivity molecule detection by plasmonic nanoantennas with selective binding at electromagnetic hotspots", *Nanoscale*, no. 3, 2014. DOI: 10.1039/C3NR04494G.

[4] T. Tanaka, T.-a. Yano, and R. Kato, "Nanostructure-enhanced infrared spectroscopy", *Nanophotonics*, vol. 11, no. 11, 2021. DOI: 10.1515/nanoph-2021-0661.

[5] J. Kim, K. Han, and J. W. Hahn, "Selective dual-band metamaterial perfect absorber for infrared stealth technology", *Scientific Reports*, vol. 7, art. no. 6740, 2017. DOI: 10.1038/s41598-017-06749-0.

[6] A. Attariabad, A. Pourziad, and M. Bemani, "A tunable and compact footprint plasmonic metasurface integrated graphene photodetector using modified omega-shaped nanoantennas", *Optics & Laser Technology*, vol. 147, art. 107660, 2022. DOI: 10.1016/j.optlastec.2021.107660.

[7] M. Ye and K. B. Crozier, "Metasurface with metallic nanoantennas and graphene nanoslits for sensing of protein monolayers and sub-monolayers", *Optics Express*, vol. 28, no. 12, pp. 18479–18492, 2020. DOI: 10.1364/OE.394564.

[8] Q. Hong *et al.*, "Hybrid metal-graphene plasmonic sensor for multi-spectral sensing in both near- and mid-infrared ranges", *Optics Express*, vol. 27, no. 24, pp. 35914–35924, 2019. DOI: 10.1364/OE.27.035914.

[9] S. A. Miandoab and R. Talebzadeh, "Ultra-sensitive and selective 2D hybrid highly doped semiconductor-graphene biosensor based on SPR and SEIRA effects in the wide range of infrared spectral", *Optical Materials*, vol. 129, art. 112572, 2022. DOI: 10.1016/j.optmat.2022.112572.

[10] D. Rodrigo *et al.*, "Mid-infrared plasmonic biosensing with graphene", *Science*, vol. 349, no. 6244, pp. 165–168, 2015. DOI: 10.1126/science.aab2051.

[11] H. Durmaz, Y. Li, and A. E. Cetin, "A multiple-band perfect absorber for SEIRA applications", *Sensors and Actuators B: Chemical*, vol. 275, pp. 174–179, 2018. DOI: 10.1016/j.snb.2018.08.053.

[12] S. Gupta, T. Arora, D. Singh, and K. K. Singh, "Nature inspired golden spiral super-ultra wideband microstrip antenna", in *Proc. of 2018 Asia-Pacific Microwave Conference (APMC)*, 2018, pp. 1603–1605. DOI: 10.23919/APMC.2018.8617550.

[13] E. Froes *et al.*, "Monopole directional antenna bioinspired in elliptical leaf with golden ratio for WLAN and 4G applications", *Scientific Reports*, vol. 12, art. no. 18654, 2022. DOI: 10.1038/s41598-022-21733-z.

[14] A. Meena, A. Garhwal, and K. Ray, "Nature Inspired Fibonacci sequence microstrip patch antenna for energy harvesting applications", *International Journal of Recent Technology and Engineering (IJRTE)*, vol. 8, no. 2, pp. 6154–6160, 2019. DOI: 10.35940/ijrte.B3761.078219.

[15] H. Abdollahi, A. Kari, and F. Samaeifar, "Detection of 2,4-dinitrotoluene by graphene oxide: First principles study", *Materials Research Express*, vol. 5, no. 5, 2018. DOI: 10.1088/2053-1591/aac1e1.

[16] H. Zhou *et al.*, "Detection of three common organic explosives using capillary electrophoresis", *Journal of Materials Science and Chemical Engineering*, vol. 4, no. 6, pp. 17–25, 2016. DOI: 10.4236/msce.2016.46003.

[17] A. Dargahi, M. Vosoughi, S. A. Mokhtari, Y. Vaziri, and M. Alighadri, "Electrochemical degradation of 2,4-Dinitrotoluene (DNT) from aqueous solutions using three-dimensional electrocatalytic reactor (3DER): Degradation pathway, evaluation of toxicity and optimization using RSM-CCD", *Arabian Journal of Chemistry*, vol. 15, no. 3, art. 103648, 2022. DOI: 10.1016/j.arabjc.2021.103648.

[18] B. Paull, C. Roux, M. Dawson, and P. Doble, "Rapid screening of selected organic explosives by high performance liquid chromatography using reversed-phase monolithic columns", *J. Forensic Sci.*, vol. 49, no. 6, pp. 1181–1186, 2004. DOI: 10.1520/JFS2004072.

[19] J. A. Mathis and B. R. McCord, "The analysis of high explosives by liquid chromatography/electrospray ionization mass spectrometry: Multiplexed detection of negative ion adducts", *Rapid Communications in Mass Spectrometry*, vol. 19, no. 2, pp. 99–104, 2004. DOI: 10.1002/rcm.1752.

[20] E. D. Palik, *Handbook of Optical Constants of Solids*. Academic Press, 1985. DOI: 10.1016/C2009-0-20920-2.

[21] G. W. Hanson, "Dyadic Green's functions and guided surface waves for a surface conductivity model of graphene", *Journal of Applied Physics*, vol. 103, art. 064302, 2008. DOI: 10.1063/1.2891452.

[22] V. P. Gusynin, S. G. Sharapov, and J. P. Carbotte, "Magneto-optical conductivity in graphene", *Journal of Physics: Condensed Matter*, vol. 19, no. 2, 2007. DOI: 10.1088/0953-8984/19/2/026222.

[23] L. Cui, J. Wang, and M. Sun, "Graphene plasmon for optoelectronics", *Reviews in Physics*, vol. 6, art. 100054, 2021. DOI: 10.1016/j.revip.2021.100054.

[24] X. Zheng, G. A. E. Vandenbosch, and V. V. Moshchalkov, "Understanding the physical behavior of plasmonic antennas through computational electromagnetics", in *Nanoplasmonics - Fundamentals and Applications*. IntechOpen, 2017, pp. 117–140. DOI: 10.5772/67589.

[25] A. Fabas *et al.*, "Dispersion-based intertwined SEIRA and SPR effect detection of 2,4-dinitrotoluene using a plasmonic metasurface", *Optics Express*, vol. 28, no. 26, pp. 39595–39605, 2020. DOI: 10.1364/OE.413325.